

Simultaneous Distributed Sensor Self-Localization and Target Tracking Using Belief Propagation and Likelihood Consensus

Florian Meyer, Erwin Riegler, Ondrej Hlinka, and Franz Hlawatsch

Institute of Telecommunications, Vienna University of Technology, Austria (florian.meyer@tuwien.ac.at)

Abstract—We introduce the framework of *cooperative simultaneous localization and tracking* (CoSLAT), which provides a consistent combination of cooperative self-localization (CSL) and distributed target tracking (DTT) in sensor networks without a fusion center. CoSLAT extends simultaneous localization and tracking (SLAT) in that it uses also intersensor measurements. Starting from a factor graph formulation of the CoSLAT problem, we develop a particle-based, distributed message passing algorithm for CoSLAT that combines nonparametric belief propagation with the likelihood consensus scheme. The proposed CoSLAT algorithm improves on state-of-the-art CSL and DTT algorithms by exchanging probabilistic information between CSL and DTT. Simulation results demonstrate substantial improvements in both self-localization and tracking performance.

Index Terms—Distributed target tracking, cooperative localization, CoSLAT, nonparametric belief propagation, likelihood consensus.

I. INTRODUCTION

Two important inference tasks in decentralized sensor networks are cooperative self-localization (CSL) [1], [2] and distributed target tracking (DTT) [3]. In CSL, each sensor acquires measurements of its own location relative to neighboring sensors, and it cooperates with all the other sensors to estimate its own location. Existing CSL algorithms include nonparametric belief propagation (NBP) [4] and other message passing algorithms [2], [5]. In DTT, each sensor acquires a measurement that is related to the state of a target, and it cooperatively estimates the target state based on the measurements of all sensors. Existing DTT algorithms include consensus-based distributed particle filters [6]–[8]. In the framework of distributed *simultaneous localization and tracking* (SLAT) [9], the sensors simultaneously track a target and localize themselves, however without using intersensor distance measurements. Methods for SLAT were proposed in [9]–[14].

CSL and DTT are closely related since (i) to contribute to DTT, a sensor needs to have information of its own location, and (ii) the accuracy of CSL may be improved if the sensors possess estimates of the state of a target. This observation motivates the development of combined CSL-DTT methods.

Here, we introduce the framework of *cooperative simultaneous localization and tracking* (CoSLAT), which, for the first time, provides a consistent combination of CSL and DTT.

This work was supported by the Austrian Science Fund (FWF) under Award S10603 (Statistical Inference) within the National Research Network SISE and by the WWTF under Award ICT10-066 (NOWIRE).

CoSLAT extends SLAT in that it uses also intersensor distance measurements. We propose a particle-based, distributed CoSLAT algorithm that integrates DTT in NBP-based CSL [2], [4], [15]. A fundamental problem—the nonavailability of essential information at the sensors—is solved by using the likelihood consensus (LC) scheme [6], [16]. The algorithm’s main new feature is a probabilistic information transfer between CSL and DTT, which allows CSL and DTT to support each other. As we will demonstrate, this leads to improved performance of both sensor localization and target tracking.

This paper is organized as follows. The system model is described in Section II. In Section III, the CoSLAT problem is defined and a basic message passing scheme for CoSLAT is derived. This scheme is further developed into a distributed CoSLAT algorithm in Section IV. Finally, simulation results are presented in Section V.

II. SYSTEM MODEL

We consider a sensor network consisting of K cooperating sensor nodes and a noncooperative target node, as depicted in Fig. 1. The set of all nodes is $\mathcal{A} = \{0, \dots, K\}$, with $k = 0$ indexing the target and $k \in \mathcal{A}_{\sim 0} \triangleq \mathcal{A} \setminus \{0\}$ indexing the sensors. Sensors and target may be mobile. The *state* of sensor or target $k \in \mathcal{A}$ at time $n \in \{0, 1, \dots\}$, denoted by $\mathbf{x}_{k,n}$, consists of the current location and, possibly, additional motion parameters such as velocity [17]. The states $\mathbf{x}_{k,n}$ evolve according to the state transition probability density functions (pdfs) $f(\mathbf{x}_{k,n}|\mathbf{x}_{k,n-1})$ and the state priors $f(\mathbf{x}_{k,0})$.

The communication and measurement topologies are described by sets \mathcal{C}_n , $\mathcal{M}_{k,n}$, and \mathcal{T}_n as follows. Two sensors $k, l \in \mathcal{A}_{\sim 0}$ are able to communicate with each other if $(k, l) \in \mathcal{C}_n \subseteq \mathcal{A}_{\sim 0} \times \mathcal{A}_{\sim 0}$. \mathcal{C}_n is symmetric, i.e., if $(k, l) \in \mathcal{C}_n$ then $(l, k) \in \mathcal{C}_n$. Sensor $k \in \mathcal{A}_{\sim 0}$ acquires a measurement $y_{k,l;n}$ relative to sensor $l \in \mathcal{A}_{\sim 0}$, with $(k, l) \in \mathcal{C}_n$, if $l \in \mathcal{M}_{k,n} \subseteq$

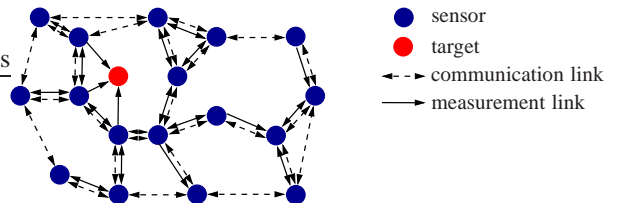


Fig. 1. Wireless sensor network with target, communication links, and measurement links.

$\mathcal{A} \setminus \{k\}$. Sensor $k \in \mathcal{A}_{\sim 0}$ acquires a measurement $y_{k,0;n}$ relative to the target, i.e., $0 \in \mathcal{M}_{k,n}$, if $k \in \mathcal{T}_n \subseteq \mathcal{A}_{\sim 0}$; i.e., $\mathcal{T}_n \triangleq \{k \in \mathcal{A}_{\sim 0} | 0 \in \mathcal{M}_{k,n}\}$. The sets \mathcal{C}_n , $\mathcal{M}_{k,n}$, and \mathcal{T}_n may be time-dependent. An example of communication and measurement topologies is given in Fig. 1. We consider a two-dimensional (2D) scenario and noisy distance measurements

$$y_{k,l;n} = \|\tilde{\mathbf{x}}_{k,n} - \tilde{\mathbf{x}}_{l,n}\| + v_{k,l;n}, \quad (1)$$

where $\tilde{\mathbf{x}}_{k,n} \triangleq [x_{1,k,n} \ x_{2,k,n}]^T$ represents the location of sensor or target k (note that this is a part of the state $\mathbf{x}_{k,n}$). The measurement noise $v_{k,l;n}$ is not necessarily Gaussian; its variance σ_v^2 is assumed known; and $v_{k,l;n}$ and $v_{k',l',n'}$ are assumed independent unless $(k, l, n) = (k', l', n')$. We note that other measurement models could be used, and the extension to the 3D case is straightforward.

III. A MESSAGE PASSING SCHEME

We first define the CoSLAT problem and derive a message passing scheme for CoSLAT. This scheme will be developed into a distributed CoSLAT algorithm in Section IV.

In CoSLAT, at time n , each sensor $k \in \mathcal{A}_{\sim 0}$ estimates both its own state $\mathbf{x}_{k,n}$ and the target state $\mathbf{x}_{0,n}$, using all the inter-sensor and sensor-target distance measurements up to time n , i.e., $\mathcal{Y}_{1:n} \triangleq \{y_{k,l;n'}\}_{k \in \mathcal{A}_{\sim 0}, l \in \mathcal{M}_{k,n'}, n' \in \{1, \dots, n\}}$. In particular, the minimum mean square error (MMSE) estimator [18] of state $\mathbf{x}_{k,n}$ is given by

$$\hat{\mathbf{x}}_{k,n}^{\text{MMSE}} \triangleq \mathbb{E}\{\mathbf{x}_{k,n} | \mathcal{Y}_{1:n}\} = \int \mathbf{x}_{k,n} f(\mathbf{x}_{k,n} | \mathcal{Y}_{1:n}) d\mathbf{x}_{k,n}, \quad (2)$$

for all $k \in \mathcal{A}$. Compared to ‘‘pure CSL’’ [2], [4], [5], [15] and ‘‘pure DTT’’ [6]–[8], the measurement set $\mathcal{Y}_{1:n}$ is extended in that it includes also the respective other measurements (i.e., sensor-target distance measurements for the sensor state estimates $\hat{\mathbf{x}}_{k,n}^{\text{MMSE}}$, $k \in \mathcal{A}_{\sim 0}$ and intersensor distance measurements for the target state estimate $\hat{\mathbf{x}}_{0,n}^{\text{MMSE}}$).

The marginal posterior pdf $f(\mathbf{x}_{k,n} | \mathcal{Y}_{1:n})$ involved in (2) can be calculated by marginalization of the joint posterior pdf $f(\mathcal{X}_{0:n} | \mathcal{Y}_{1:n})$ of the past and present states of all sensors and the target, $\mathcal{X}_{0:n} \triangleq \{\mathbf{x}_{k,n'}\}_{k \in \mathcal{A}, n' \in \{0, \dots, n\}}$. By using Bayes’ rule and common assumptions [2], one can show that this joint posterior pdf factorizes as follows:

$$f(\mathcal{X}_{0:n} | \mathcal{Y}_{1:n}) \propto \left[\prod_{k \in \mathcal{A}} f(\mathbf{x}_{k,0}) \right] \prod_{n'=1}^n \left[\prod_{k' \in \mathcal{A}} f(\mathbf{x}_{k',n'} | \mathbf{x}_{k',n'-1}) \right] \times \prod_{l \in \mathcal{M}_{k',n'}} f(y_{k',l;n'} | \mathbf{x}_{k',n'}, \mathbf{x}_{l,n'}). \quad (3)$$

Calculating $f(\mathbf{x}_{k,n} | \mathcal{Y}_{1:n})$ by straightforward marginalization is infeasible. However, an approximation of the marginal posterior, $b_{k,n}(\mathbf{x}_{k,n}) \approx f(\mathbf{x}_{k,n} | \mathcal{Y}_{1:n})$, can be obtained by executing iterative belief propagation message passing [19] on the factor graph corresponding to the factorization (3), which is shown in Fig. 2. At each time n , P message passing iterations are performed. Extending the belief propagation message passing scheme for distributed CSL proposed in [2] to include a non-cooperative target, the iterated approximate marginal posterior

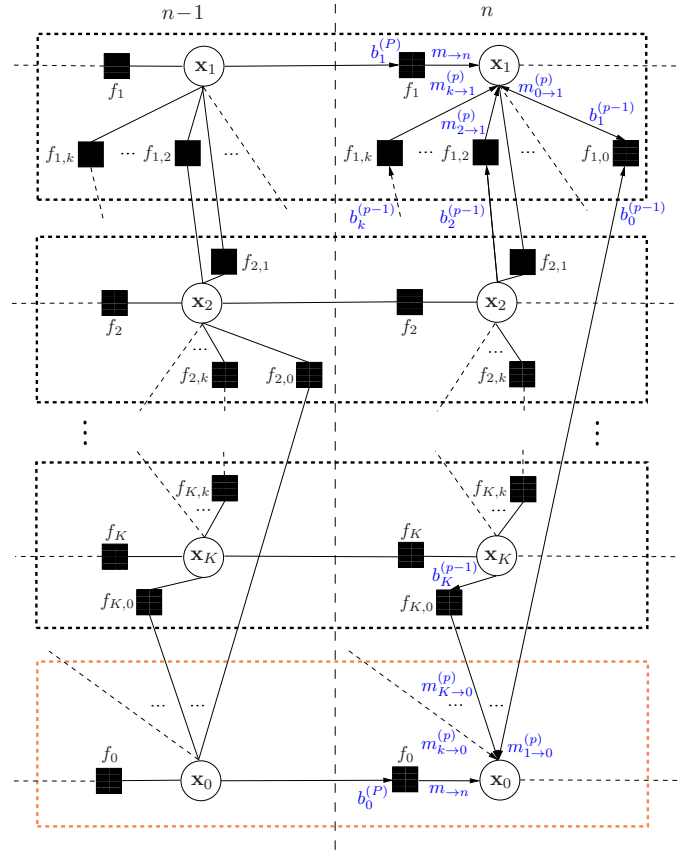


Fig. 2. Factor graph for CoSLAT, with sensors $k \in \{1, \dots, K\}$ and a target ($k \in 0$). We use the short notation $f_k \triangleq f(\mathbf{x}_{k,n'} | \mathbf{x}_{k,n'-1})$ and $f_{k,l} \triangleq f(y_{k,l;n'} | \mathbf{x}_{k,n'}, \mathbf{x}_{l,n'})$, for $n' \in \{1, \dots, n\}$. The upper (black) dotted boxes correspond to the CSL part; the bottom (red) dotted box corresponds to the DTT part. All time indices are omitted for simplicity. Only the messages and approximate marginal posteriors involved in calculating $b_{1,n}(\mathbf{x}_{1,n})$ and $b_{0,n}(\mathbf{x}_{0,n})$ are shown. Edges between black dotted boxes imply communication.

(AMP) of sensor or target node $k \in \mathcal{A}$ at message passing iteration p , $b_{k,n}^{(p)}(\mathbf{x}_{k,n})$, is obtained as

$$b_{k,n}^{(p)}(\mathbf{x}_{k,n}) \propto \begin{cases} m_{\rightarrow n}(\mathbf{x}_{k,n}) \prod_{l \in \mathcal{M}_{k,n}} m_{l \rightarrow k}^{(p)}(\mathbf{x}_{k,n}), & k \in \mathcal{A}_{\sim 0} \\ m_{\rightarrow n}(\mathbf{x}_{0,n}) \prod_{l \in \mathcal{T}_n} m_{l \rightarrow 0}^{(p)}(\mathbf{x}_{0,n}), & k = 0, \end{cases} \quad (4)$$

with the ‘‘prediction message’’

$$m_{\rightarrow n}(\mathbf{x}_{k,n}) \triangleq \int f(\mathbf{x}_{k,n} | \mathbf{x}_{k,n-1}) b_{k,n-1}^{(p)}(\mathbf{x}_{k,n-1}) d\mathbf{x}_{k,n-1} \quad (5)$$

and the ‘‘measurement messages’’

$$m_{l \rightarrow k}^{(p)}(\mathbf{x}_{k,n}) \triangleq \begin{cases} \int f(y_{k,l;n} | \mathbf{x}_{k,n}, \mathbf{x}_{l,n}) b_{l,n}^{(p-1)}(\mathbf{x}_{l,n}) d\mathbf{x}_{l,n}, & k \in \mathcal{A}_{\sim 0}, l \in \mathcal{A}_{\sim 0} \\ \int f(y_{k,0;n} | \mathbf{x}_{k,n}, \mathbf{x}_{0,n}) n_{0 \rightarrow k}^{(p-1)}(\mathbf{x}_{0,n}) d\mathbf{x}_{0,n}, & k \in \mathcal{A}_{\sim 0}, l = 0 \\ \int f(y_{l,0;n} | \mathbf{x}_{0,n}, \mathbf{x}_{l,n}) n_{l \rightarrow 0}^{(p-1)}(\mathbf{x}_{l,n}) d\mathbf{x}_{l,n}, & k = 0, l \in \mathcal{A}_{\sim 0}, \end{cases} \quad (6)$$

where $n_{l \rightarrow 0}^{(p-1)}(\mathbf{x}_{l,n})$ and $n_{0 \rightarrow k}^{(p-1)}(\mathbf{x}_{0,n})$ (constituting the ‘‘extrinsic information’’) are given by

$$\begin{aligned} n_{l \rightarrow 0}^{(p-1)}(\mathbf{x}_{l,n}) &= m_{\rightarrow n}(\mathbf{x}_{l,n}) \prod_{k' \in \mathcal{M}_{l,n} \setminus \{0\}} m_{k' \rightarrow l}^{(p-1)}(\mathbf{x}_{l,n}) \\ n_{0 \rightarrow k}^{(p-1)}(\mathbf{x}_{0,n}) &= m_{\rightarrow n}(\mathbf{x}_{0,n}) \prod_{k' \in \mathcal{T}_n \setminus \{k\}} m_{k' \rightarrow 0}^{(p-1)}(\mathbf{x}_{0,n}). \end{aligned} \quad (7)$$

However, in the proposed CoSLAT algorithm, we modify (6) in that we approximate the extrinsic information by the corresponding AMP. This leads to the following approximation for the measurement messages:

$$m_{l \rightarrow k}^{(p)}(\mathbf{x}_{k,n}) \approx \begin{cases} \int f(y_{k,l;n} | \mathbf{x}_{k,n}, \mathbf{x}_{l,n}) b_{l,n}^{(p-1)}(\mathbf{x}_{l,n}) d\mathbf{x}_{l,n}, & k \in \mathcal{A} \sim 0 \\ \int f(y_{l,0;n} | \mathbf{x}_{0,n}, \mathbf{x}_{l,n}) b_{l,n}^{(p-1)}(\mathbf{x}_{l,n}) d\mathbf{x}_{l,n}, & k = 0, \end{cases} \quad (8)$$

for all $l \in \mathcal{A}$. In this way, the costly calculation of the extrinsic information (7) is avoided. Numerical analysis showed that although this approximation leads to slightly overconfident AMPs, the estimation performance is not affected.

Because according to (1), $y_{k,l;n}$ depends only on the locations of (sensor or target) nodes k and l , $m_{l \rightarrow k}^{(p)}(\mathbf{x}_{k,n})$ is 2D regardless of the dimension of $\mathbf{x}_{k,n}$. The messages and AMPs needed for calculating $b_{1,n}^{(p)}(\mathbf{x}_{1,n})$ and $b_{0,n}^{(p)}(\mathbf{x}_{0,n})$ according to (4), (5), and (8) are depicted in Fig. 2. Messages are sent only forward in time, and iterative message passing is performed at each time step individually [2]. We do not send messages backward in time because this would cause the computation, communication, and memory requirements as well as the latency to grow linearly with time. As a consequence, $m_{\rightarrow n}(\mathbf{x}_{k,n})$ in (5) remains unchanged during the message passing iterations.

The computation of the AMPs $b_{k,n}^{(p)}(\mathbf{x}_{k,n})$ according to (4) differs from pure CSL and pure DTT. For $k = 0$ (target), the local likelihood functions used in DTT [6] are replaced by the measurement messages (8). In this way, the uncertainties about the locations of all sensors involved in DTT, $k' \in \mathcal{T}_n$, are taken into account. For $k \in \mathcal{T}_n$ (a sensor involved in DTT), also messages from the target node are considered, i.e., probabilistic information about the target location is used by the sensors for improved self-localization. This probabilistic information transfer between the CSL and DTT parts is key to the superior performance of CoSLAT.

IV. A DISTRIBUTED CoSLAT ALGORITHM

Next, we develop the message passing scheme (4), (5), and (8) into a distributed CoSLAT algorithm.

A. Nonparametric Belief Propagation

Because direct calculation of (4), (5), and (8) is still infeasible, we use an approximate implementation via NBP [4], [15]. In NBP, all AMPs and messages are represented by particles $\mathbf{x}^{(j)}$ and weights $w^{(j)}$, for $j \in \{1, \dots, J\}$. This particle representation is also suited to multimodal AMPs and

messages. NBP can be viewed as an extension of particle filtering to factor graphs with loops. In a CSL scenario, it exhibits fast convergence and high accuracy [2]. An algorithmic description of NBP for CSL can be found in [4], [15]; the extension to our CoSLAT setting is straightforward. In the CoSLAT message passing scheme, all particles representing a message have equal weights, i.e., $w^{(j)} \equiv 1/J$.

In addition to the particle representation of messages, NBP uses an approximate kernel representation that can be easily derived from the particle representation. This kernel representation provides a closed-form expression that can be evaluated at any given point. This is necessary for performing the message multiplication in (4) and for using the LC (see Section IV-B). Given a set of particles and weights $\{(\mathbf{x}^{(j)}, w^{(j)})\}_{j=1}^J$ representing a measurement message $m(\mathbf{x})$, the kernel representation of $m(\mathbf{x})$ is obtained as

$$\hat{m}(\mathbf{x}) = \sum_{j=1}^J w^{(j)} K(\tilde{\mathbf{x}} - \tilde{\mathbf{x}}^{(j)}), \quad (9)$$

where, as before, the 2D vector $\tilde{\mathbf{x}}$ denotes the location part of the state \mathbf{x} . A standard choice for the kernel $K(\tilde{\mathbf{x}})$ in the 2D localization scenario is the 2D Gaussian function $K(\tilde{\mathbf{x}}) = (2\pi\sigma_K^2)^{-1} \exp(-\|\tilde{\mathbf{x}}\|^2/(2\sigma_K^2))$. The variance σ_K^2 is usually estimated from the particles and weights. When σ_K^2 is large, $\hat{m}(\mathbf{x})$ is smooth but some of the finer details of $m(\mathbf{x})$ may be smoothed out; when σ_K^2 is small, $\hat{m}(\mathbf{x})$ preserves more of these fine details but may exhibit some artificial structure not present in $m(\mathbf{x})$ [15], [20].

B. Likelihood Consensus Based Computation of $b_{0,n}^{(p)}(\mathbf{x}_{0,n})$

In CSL, the NBP message passing scheme can be performed in a distributed manner using only local intersensor communications. With CoSLAT, a distributed implementation is complicated by the fact that the target node is noncooperative and therefore some vital information is not communicated to the sensors. More specifically, calculating the AMP of the target state, $b_{0,n}^{(p)}(\mathbf{x}_{0,n})$, according to (4) requires the product of measurement messages $\prod_{l \in \mathcal{T}_n} m_{l \rightarrow 0}^{(p)}(\mathbf{x}_{0,n})$. Unfortunately, this message product is not available at the sensors.

We solve this problem by using the LC scheme, which was proposed in a different context in [6]. Consider a sensor $l \in \mathcal{T}_n$ and the kernel approximation $\hat{m}_{l \rightarrow 0}^{(p)}(\mathbf{x}_{0,n})$ (see (9)) of the measurement message $m_{l \rightarrow 0}^{(p)}(\mathbf{x}_{0,n})$, which was calculated at sensor l . Following the LC principle, the logarithm of $\hat{m}_{l \rightarrow 0}^{(p)}(\mathbf{x}_{0,n})$ is approximated by a finite-order basis expansion:

$$\log \hat{m}_{l \rightarrow 0}^{(p)}(\mathbf{x}_{0,n}) \approx \sum_{r=1}^R \beta_{l;n,r}^{(p)}(y_{l,0;n}) \varphi_r(\mathbf{x}_{0,n}). \quad (10)$$

Here, the basis functions $\varphi_r(\mathbf{x}_{0,n})$ do not depend on l , i.e., the same set of basis functions is used by all sensors. The expansion coefficients $\beta_{l;n,r}^{(p)}(y_{l,0;n})$, $r \in \{1, \dots, R\}$ can be calculated locally at sensor l by least squares fitting using the particles of the prediction message $m_{\rightarrow n}(\mathbf{x}_{l,n})$ as reference points (cf. [6]). Furthermore, we formally set $\beta_{l;n,r}^{(p)}(y_{l,0;n}) = 0$ for all $r \in \{1, \dots, R\}$ if $l \notin \mathcal{T}_n$.

The local approximations (10) entail the following approximation of the desired message product:

$$\begin{aligned} \prod_{l \in \mathcal{T}_n} \hat{m}_{l \rightarrow 0}^{(p)}(\mathbf{x}_{0,n}) &\approx \prod_{l \in \mathcal{T}_n} \exp\left(\sum_{r=1}^R \beta_{l;n,r}^{(p)}(y_{l,0;n}) \varphi_r(\mathbf{x}_{0,n})\right) \\ &= \exp\left(\sum_{r=1}^R B_{n,r}^{(p)} \varphi_r(\mathbf{x}_{0,n})\right), \end{aligned} \quad (11)$$

with

$$B_{n,r}^{(p)} \triangleq \sum_{l \in \mathcal{T}_n} \beta_{l;n,r}^{(p)}(y_{l,0;n}) = \sum_{l \in \mathcal{A}_{\sim 0}} \beta_{l;n,r}^{(p)}(y_{l,0;n}), \quad (12)$$

where the last equation follows because $\beta_{l;n,r}^{(p)}(y_{l,0;n}) = 0$ for all $l \notin \mathcal{T}_n$. The coefficients $B_{n,r}^{(p)}$ in (12) can be computed at each sensor by running R parallel instances of an average consensus algorithm or a gossip algorithm [21], [22]. This requires only local communications between neighboring sensors. After convergence of the consensus or gossip algorithms, an approximation of the functional form of $\prod_{l \in \mathcal{T}_n} \hat{m}_{l \rightarrow 0}^{(p)}(\mathbf{x}_{0,n})$ is available at each sensor. Each sensor is then able to calculate a particle representation of $m_{\rightarrow n}(\mathbf{x}_{0,n}) \prod_{l \in \mathcal{T}_n} \hat{m}_{l \rightarrow 0}^{(p)}(\mathbf{x}_{0,n}) \approx b_{0,n}^{(p)}(\mathbf{x}_{0,n})$ (see (4)) based on the importance sampling principle [23]. More specifically, weights $\{w_{0,n}^{(j)}\}_{j=1}^J$ associated with the particles $\{\mathbf{x}_{0,n}^{(j)}\}_{j=1}^J$ representing $m_{\rightarrow n}(\mathbf{x}_{0,n})$ are obtained by evaluating the approximation (11) of $\prod_{l \in \mathcal{T}_n} \hat{m}_{l \rightarrow 0}^{(p)}(\mathbf{x}_{0,n})$ at the $\mathbf{x}_{0,n}^{(j)}$, i.e., by calculating $w_{0,n}^{(j)} = \exp\left(\sum_{r=1}^R B_{n,r}^{(p)} \varphi_r(\mathbf{x}_{0,n}^{(j)})\right)$ for all $j \in \{1, \dots, J\}$. Then, a resampling step [23] is performed to obtain equally weighted particles representing $b_{0,n}^{(p)}(\mathbf{x}_{0,n})$.

Once a particle approximation of $b_{0,n}^{(p)}(\mathbf{x}_{0,n})$ is available at each sensor, computations in the CSL part of the factor graph (cf. the upper dotted boxes in Fig. 2) at message passing iteration $p+1$ can be performed in a distributed way using NBP as described in [4], [15]. Thus, each sensor $k \in \mathcal{A}_{\sim 0}$ is able to calculate approximate marginals of its own state $\mathbf{x}_{k,n}$ and of the target state $\mathbf{x}_{0,n}$ by means of the NBP implementation of (4), (5), and (8), using information that is either locally available or obtained through local communication.

V. SIMULATION RESULTS

We consider a network of $K=7$ sensors, of which four are mobile sensors and three are anchors (i.e., static sensors with perfect location information modeled via Dirac-shaped priors). The sensors are placed within a field of size 50×50 . Each sensor has a communication range of 56 and localizes itself and the target. We consider two scenarios. In scenario 2, which is shown in Fig. 3, the upper-right and lower-left sensors have a measurement radius of 20, and therefore, initially (at time $n=0$), they do not have enough partners for self-localization. With conventional CSL, at $n=0$, these sensors have a multimodal marginal posterior and are thus unable to localize themselves. The measurement regions of the other five sensors cover the entire field. Scenario 1 differs from scenario 2 in that also the lower-left sensor covers the entire field.

The states of the mobile sensors and the target consist of location and velocity, i.e., $\mathbf{x}_{k,n} = [x_{1,k,n} \ x_{2,k,n} \ \dot{x}_{1,k,n} \ \dot{x}_{2,k,n}]^T$.

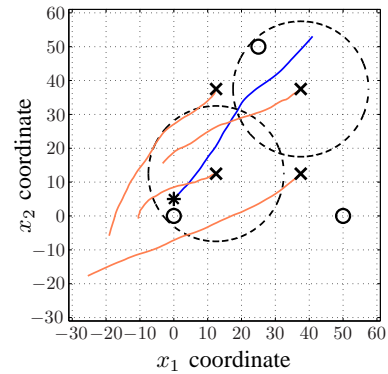


Fig. 3. Network topology used for the simulations, along with a realization of the target and sensor trajectories. Initial mobile sensor locations are indicated by crosses, anchor locations by circles, and the initial target location by a star. The big dashed circles indicate the measurement regions of the upper-right sensor (in both scenarios) and of the lower-left sensor (in scenario 2).

Mobile sensor trajectories are created by using a Dirac-shaped location prior at the locations indicated in Fig. 3. However, in the simulations of the algorithms, all mobile sensors have a location prior that is uniform on $[-500, 500] \times [-500, 500]$. Furthermore, we used a Gaussian sensor velocity prior with mean $\boldsymbol{\mu}_{k,0} = [-0.1 \ -0.1]^T$ and covariance matrix $\mathbf{C}_{k,0} = \text{diag}\{0.1, 0.1\}$ and a Gaussian target state prior with mean $\boldsymbol{\mu}_{0,0} = [0 \ 5 \ 0.4 \ 0.4]^T$ and covariance matrix $\mathbf{C}_{0,0} = \text{diag}\{1, 1, 0.001, 0.001\}$. The mobile sensors and the target evolve independently according to $\mathbf{x}_{k,n} = \mathbf{G}\mathbf{x}_{k,n-1} + \mathbf{W}\mathbf{u}_{k,n}$, $n=1, 2, \dots$ [17], where the matrices $\mathbf{G} \in \mathbb{R}^{4 \times 4}$ and $\mathbf{W} \in \mathbb{R}^{4 \times 2}$ are chosen as in [6] and the driving noise vectors $\mathbf{u}_{k,n} \in \mathbb{R}^2$ are Gaussian, i.e., $\mathbf{u}_{k,n} \sim \mathcal{N}(\mathbf{0}, \sigma_u^2 \mathbf{I})$, with variance $\sigma_u^2 = 0.0005$ and with $\mathbf{u}_{k,n}$ and $\mathbf{u}_{k',n'}$ independent unless $(k,n) = (k',n')$. We performed 500 simulation runs. In each run, the sensors and the target move along the specific trajectory realizations shown in Fig. 3. The observation noise variance is $\sigma_v^2 = 2$. Each mobile sensor starts moving only when it is sufficiently localized in the sense that the sum of its estimated location coordinate variances is below $5\sigma_v^2$.

We compare the performance of the proposed CoSLAT algorithm with that of a state-of-the-art reference method, which separately performs CSL by means of NBP as described in [15] and DTT by means of the LC-based distributed particle filter presented in [6]. The DTT method uses the sensor location estimates provided by the CSL method. In both the CoSLAT method and the reference method, the LC scheme uses an average consensus [21] with five iterations, and the basis expansion is a third-order polynomial approximation [6], resulting in an expansion order of $R=16$. The NBP scheme performs $P=3$ message passing iterations. The kernel variance for the measurement messages (cf. (9)) is chosen as $\sigma_K^2 = \sigma_v^2$, as recommended in [4]. The number of particles used by both NBP and the distributed particle filter is $J=500$.

Fig. 4 shows the simulated root-mean-square self-localization and target localization errors for $n=0, \dots, 75$. These errors were determined by averaging over all sensors and all simulation runs. In scenario 1, for $n > 43$, the self-localization error of CoSLAT is seen to be significantly smaller than that of the reference method. This is because with pure

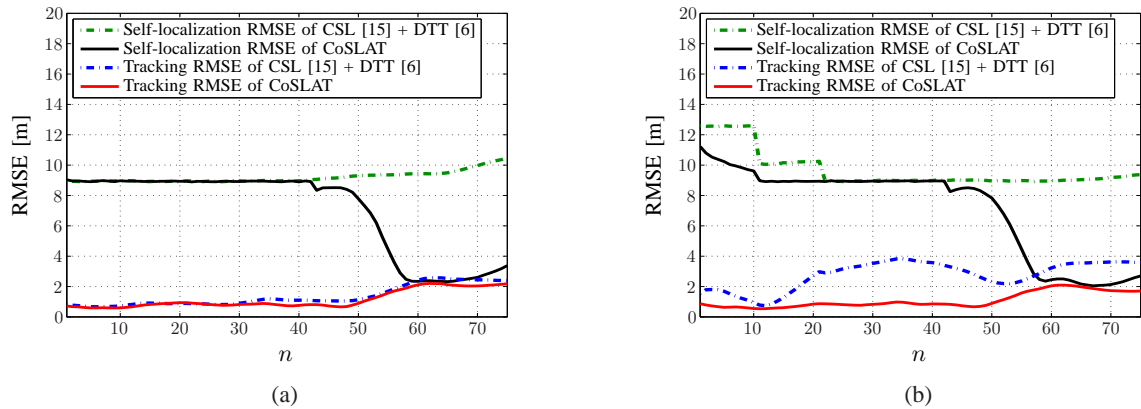


Fig. 4. Average root-mean-square errors (RMSE) of sensor self-localization and target tracking versus time n , for (a) scenario 1 and (b) scenario 2.

CSL, the upper-right sensor has not enough partners for self-localization, whereas with CoSLAT, for $n > 43$, the upper-right sensor can use the measurement of its distance to the target to calculate the message from the target node, $m_{0 \rightarrow k}^{(p)}(\mathbf{x}_{k,n})$, and use this additional information to improve its self-localization performance. The tracking performance of CoSLAT in scenario 1 is similar to that of the reference method.

In scenario 2, for $n > 43$, the self-localization error of CoSLAT is again much smaller than that of the reference method. In addition, it is also smaller for $n < 22$. This is because in scenario 2, for $n < 22$, also the lower-left sensor has not enough partners for self-localization when pure CSL is used. Furthermore, the target tracking error of CoSLAT is now significantly smaller than that of the reference method for almost all times. This is because with separate CSL and DTT, the poor self-localization of the lower-left sensor at $n < 22$ degrades the target tracking performance. This higher target tracking error is retained for $n \geq 22$ even when all sensors involved in the target tracking are well localized.

VI. CONCLUSION

The novel framework of *cooperative simultaneous localization and tracking* (CoSLAT) provides a complete and consistent combination of cooperative self-localization (CSL) and distributed target tracking (DTT). Starting from a factor graph formulation of the CoSLAT problem, we developed a particle-based, distributed message passing algorithm for CoSLAT that performs a probabilistic information transfer between CSL and DTT. Simulation results demonstrated significant improvements in both self-localization and target tracking performance compared to state-of-the-art algorithms.

ACKNOWLEDGMENT

The authors would like to thank Prof. Henk Wymeersch for illuminating comments.

REFERENCES

- [1] N. Patwari, J. N. Ash, S. Kyperountas, A. O. Hero III, R. L. Moses, and N. S. Correal, "Locating the nodes: Cooperative localization in wireless sensor networks," *IEEE Signal Process. Mag.*, vol. 22, pp. 54–69, Jul. 2005.
- [2] H. Wymeersch, J. Lien, and M. Z. Win, "Cooperative localization in wireless networks," *Proc. IEEE*, vol. 97, pp. 427–450, Feb. 2009.
- [3] J. Liu, M. Chu, and J. Reich, "Multitarget tracking in distributed sensor networks," *IEEE Signal Process. Mag.*, vol. 24, pp. 36–46, May 2007.
- [4] A. T. Ihler, J. W. Fisher, R. L. Moses, and A. S. Willsky, "Nonparametric belief propagation for self-localization of sensor networks," *IEEE J. Sel. Areas Comm.*, vol. 23, pp. 809–819, Apr. 2005.
- [5] C. Pedersen, T. Pedersen, and B. H. Fleury, "A variational message passing algorithm for sensor self-localization in wireless networks," in *Proc. IEEE ISIT-11*, Saint Petersburg, Russia, pp. 2158–2162, Aug. 2011.
- [6] O. Hlinka, O. Slučiak, F. Hlawatsch, P. M. Djurić, and M. Rupp, "Likelihood consensus and its application to distributed particle filtering," *IEEE Trans. Signal Process.*, vol. 60, pp. 4334–4349, Aug. 2012.
- [7] S. Farahmand, S. I. Roumeliotis, and G. B. Giannakis, "Set-membership constrained particle filter: Distributed adaptation for sensor networks," *IEEE Trans. Signal Process.*, vol. 59, pp. 4122–4138, Sep. 2011.
- [8] V. Savic, H. Wymeersch, and S. Zazo, "Belief consensus algorithms for distributed target tracking in wireless sensor networks," 2012. arXiv:1202.5261v1[cs.DC].
- [9] C. Taylor, A. Rahimi, J. Bachrach, H. Shrobe, and A. Grue, "Simultaneous localization, calibration, and tracking in an ad hoc sensor network," in *Proc. IPSN-06*, Nashville, TN, pp. 27–33, Apr. 2006.
- [10] S. Funiak, C. Guestrin, M. Paskin, and R. Sukthankar, "Distributed localization of networked cameras," in *Proc. IPSN-06*, Nashville, TN, pp. 34–42, Apr. 2006.
- [11] A. F. Garcia-Fernandez, M. R. Morelande, and J. Grajal, "Multitarget simultaneous localization and mapping of a sensor network," *IEEE Trans. Signal Process.*, vol. 59, pp. 4544–4558, Oct. 2011.
- [12] P. Oguz-Ekim, J. Gomes, J. Xavier, and P. Oliveira, "ML-based sensor network localization and tracking: Batch and time-recursive approaches," in *Proc. EUSIPCO-09*, Glasgow, Scotland, Aug. 2009.
- [13] X. Chen, A. Edelstein, Y. Li, M. Coates, M. Rabbat, and A. Men, "Sequential Monte Carlo for simultaneous passive device-free tracking and sensor localization using received signal strength measurements," in *Proc. IPSN-11*, Chicago, IL, pp. 342–353, Apr. 2011.
- [14] N. Kantas, S. Singh, and A. Doucet, "Distributed maximum likelihood for simultaneous self-localization and tracking in sensor networks," *IEEE Trans. Signal Process.*, vol. 60, pp. 5038–5047, Oct. 2012.
- [15] J. Lien, J. Ferner, W. Srichavengsup, H. Wymeersch, and M. Z. Win, "A comparison of parametric and sample-based message representation in cooperative localization," *Int. J. Navig. Observ.*, 2012.
- [16] O. Hlinka, F. Hlawatsch, and P. M. Djurić, "Likelihood consensus-based distributed particle filtering with distributed proposal density adaptation," in *Proc. IEEE ICASSP-12*, Kyoto, Japan, pp. 3869–3872, Mar. 2012.
- [17] X. R. Li and V. P. Jilkov, "Survey of maneuvering target tracking. Part I: Dynamic models," *IEEE Trans. Aerosp. Electron. Syst.*, vol. 39, pp. 1333–1364, Oct. 2003.
- [18] S. M. Kay, *Fundamentals of Statistical Signal Processing: Estimation Theory*. Upper Saddle River, NJ: Prentice-Hall, 1993.
- [19] F. R. Kschischang, B. J. Frey, and H.-A. Loeliger, "Factor graphs and the sum-product algorithm," *IEEE Trans. Inf. Theory*, vol. 47, pp. 498–519, Feb. 2001.
- [20] Z. Botev, "Nonparametric density estimation via diffusion mixing." The University of Queensland, Postgraduate Series, Nov. 2007. <http://espace.library.uq.edu.au/view/UQ:120006>.
- [21] R. Olfati-Saber and R. M. Murray, "Consensus problems in networks of agents with switching topology and time-delays," *IEEE Trans. Autom. Contr.*, vol. 49, pp. 1520–1533, Sep. 2004.
- [22] A. G. Dimakis, S. Kar, J. M. F. Moura, M. G. Rabbat, and A. Scaglione, "Gossip algorithms for distributed signal processing," *Proc. IEEE*, vol. 98, pp. 1847–1864, Nov. 2010.
- [23] A. Doucet, N. De Freitas, and N. Gordon, *Sequential Monte Carlo Methods in Practice*. New York, NY: Springer, 2001.